https://doi.org/10.5194/acp-2021-159
Preprint. Discussion started: 23 February 2021


Atmospheric Chemistry and Physics Discussions

# Chemical composition, optical properties, and oxidative potential of water- and methanol-soluble organic compounds emitted from the combustion of biomass materials and coal

Tao Cao[1,2], Meiju Li[1,3], Chunlin Zou[1,3], Xingjun Fan[4], Jianzhong Song[1,2,5,*], Wanglu, Jia[1,2], Chiling Yu[1,2], Zhiqiang Yu[1,2], Ping'an Peng[1,2,3,5]

[1]State Key Laboratory of Organic Geochemistry and Guangdong Provincial Key Laboratory of Environmental Protection and Resources Utilization, Guangzhou Institute of Geochemistry, Chinese Academy of Sciences, Guangzhou 510640, China

[2]CAS Center for Excellence in Deep Earth Science, Guangzhou, 510640, China

[3]University of Chinese Academy of Sciences, Beijing 100049, China

[4]College of Resource and Environment, Anhui Science and Technology University, Anhui 233100, China

[5]Guangdong-Hong Kong-Macao Joint Laboratory for Environmental Pollution and Control

*_Correspondence to_: Jianzhong Song (songjzh@gig.ac.cn)

https://doi.org/10.5194/acp-2021-159
Preprint. Discussion started: 23 February 2021


Atmospheric Chemistry and Physics Discussions


## Abstract

Biomass burning (BB) and coal combustion (CC) are important sources of brown carbon (BrC) in ambient aerosols. In this study, six biomass materials and five types of coal were combusted to generate fine smoke particles. The BrC fractions, including water-soluble organic compounds (WSOC), humic-like substances (HULIS), and methanol-soluble organic compounds (MSOC), were subsequently fractionated and their optical properties and chemical structures were then comprehensively investigated using UV-visible spectroscopy, proton nuclear magnetic resonance spectroscopy ($^1$H-NMR), and fluorescence extraction-emission matrix spectroscopy (EEM) combined with parallel factor analysis (PARAFAC). In addition, the oxidative potential (OP) of BB and CC BrC was measured with the dithiothreitol (DTT) method. The results showed that WSOC, HULIS, and MSOC accounted for 2.3%–22%, 0.5%–10%, and 6.4%–73% of the total mass of combustion-derived $PM_{2.5}$, respectively, with MSOC extracting the highest concentrations of organic compounds. The MSOC fractions had the highest light absorption capacity (mass absorption efficiency at 365 nm ($MAE_{365}$): 1.0–2.7 $m^2$/gC) for both BB and CC smoke, indicating that MSOC contained more of the strong light-absorbing components. Therefore, MSOC may better represent the total BrC than the water-soluble fractions. Some significant differences were observed between the BrC fractions emitted from BB and CC, with more water-soluble BrC fractions with higher $MAE_{365}$ and lower absorption Ångström exponent values detected in smoke emitted from BB than from CC. The EEM-PARAFAC analysis identified four fluorophores: two protein-like, one humic-like, and one polyphenol-like. The protein-like substance was the dominant component of WSOC (47%–80%), HULIS (44%–87%), and MSOC (42%–70%). The $^1$H-NMR results suggested that

https://doi.org/10.5194/acp-2021-159
Preprint. Discussion started: 23 February 2021


Atmospheric Chemistry and Physics Discussions

BB BrC contained more oxygenated aliphatic functional groups (H-C-O), whereas CC BrC contained more unsaturated fractions (H-C-C = and Ar-H). The DTT assays indicated that BB BrC generally had a stronger OP ($DTT_{mass}$, 2.6–85 pmol/min/μg) than CC BrC ($DTT_{mass}$, 0.4–11 pmol/min/μg), with MSOC having a stronger OP than WSOC and HULIS. Therefore, the BrC fractions from BB had higher OP values than those from CC.

https://doi.org/10.5194/acp-2021-159
Preprint. Discussion started: 23 February 2021


Atmospheric Chemistry and Physics Discussions

## 1. Introduction

Brown carbon (BrC) is an organic compound with strong light-absorption at ultraviolet and short-visible wavelengths, and is abundant in ambient aerosols (Chen and Bond, 2010; Laskin et al., 2015; Alexander et al., 2008), rain, cloud, and fog water (Santos et al., 2009; Santos et al., 2012; Izhar et al., 2020). Due to its strong light absorption ability, BrC can affect the radiative balance of aerosol and photochemical reactions in the atmospheric environment (Andreae and Gelencser, 2006; Kumar et al., 2018a; Nozière et al., 2011). Moreover, BrC has the ability to catalyze the generation of reactive oxygen species (ROS), which potentially have an adverse impact on human health (Bates et al., 2019; Lin and Yu, 2019; Ma et al., 2018).

Brown carbon originates from various sources, include primary emission sources, such as biomass burning (BB), coal combustion (CC), and vehicular emissions (Fan et al., 2018; Li et al., 2018; Chen et al., 2019; Sun et al., 2017); and secondary processes, such as reactions between carbonyls and ammonia or amines, as well as the photochemical transformation of volatile organic compounds (Evangeliou et al., 2019; Lin et al., 2015). Among these sources, BB and CC are considered to make significant contributions to atmospheric BrC materials, as indicated in both laboratory and field studies (Li et al., 2018; Park and Yu, 2016; van der Werf et al., 2010; Yan et al., 2015). For example, BrC fractions, such as water-soluble organic compounds (WSOC), humic-like substances (HULIS), and methanol-soluble compounds (MSOC), have been found to be abundant in fresh emissions from the burning of crop straw, wood branches, and coals of different maturity (Park and Yu, 2016; Fan et al., 2018; Li et al., 2018; Huo et al., 2018). These studies have also demonstrated that the chemical properties of primary BrC are variable due to the inherent heterogeneity and complexity of fuel materials

https://doi.org/10.5194/acp-2021-159
Preprint. Discussion started: 23 February 2021


Atmospheric Chemistry and Physics Discussions

and combustion conditions (Huo et al., 2018; Fan et al., 2018; Li et al., 2018; Atwi et al., 2021). For example, the light absorption properties of primary HULIS produced by the combustion of three crop straws under different moisture contents and stacking modes are different. The absorption Ångström exponent (AAE) increased and mass absorption efficiency at 365 nm ($MAE_{365}$) decreased under high moisture or stacking conditions (Huo et al., 2018). The water-soluble BrC emitted from low maturity CC generally had relatively lower $MAE_{365}$ values (Li et al., 2018). However, these studies only focused on the BrC fractions emitted from BB or CC, and therefore the comprehensive characterization and full understanding of the BrC fractions from combustion processes is still required. In addition, the redox activity of water-soluble organic fractions (WSOC and HULIS) and the water-insoluble organic fraction in ambient aerosols have been investigated, and all are known to be significant redox-active organic compounds associated with ROS generation, which can therefore adversely affect human health (Moufarrej et al., 2020; Bates et al., 2019; Verma et al., 2012; Kramer et al., 2016; Wong et al., 2019). As important contributors of ambient BrC, combustion-derived BrC is expected to have a strong redox activity and be harmful to human health. However, few studies have directly investigated the oxidative potential (OP) of BrC emitted from combustion processes.

Biomass fuels and coals are two traditional sources of energy in residential properties in some developing countries, especially China and India (Sun et al., 2017; Huo et al., 2018; Singh et al., 2021). Due to incomplete combustion and poor pollution control, BB and CC release various pollutants, including particulate matter (PM), elemental carbon (EC), and BrC. In this study, we investigated the optical properties, chemical composition, and OP of BrC fractions in smoke emitted from BB and CC. Six biomass materials (three crop straws and three wood

https://doi.org/10.5194/acp-2021-159
Preprint. Discussion started: 23 February 2021


Atmospheric Chemistry and Physics Discussions

93 branches) and five coals with different maturities were combusted and the resulting smoke
94 particles were collected in a laboratory combustion chamber. The water soluble (WSOC and
95 HULIS) and methanol soluble (MSOC) fractions in smoke were fractionated using pure water
96 combined with a solid-phase extraction (SPE) and methanol extraction. Subsequently, their
97 chemical and optical properties were measured using a total organic carbon analyzer, UV-
98 visible spectroscopy, fluorescence extraction-emission matrix spectroscopy (EEM) combined
99 with parallel factor analysis (PARAFAC), and proton nuclear magnetic resonance spectroscopy
100 ($^1$H-NMR). Moreover, the OP of the BrC fractions was determined by a dithiothreitol (DTT)
101 assay. The information obtained will enhance our understanding of the chemical composition,
102 light absorption, fluorophores, and OP of the primary BrC from BB and CC, and could be used
103 to estimate the environmental and climate impacts of different types of combustion-derived
104 BrC.
105
106 **2. Materials and methods**
107 **2.1. The BB and CC smoke samples**
108 In this study, six biomass materials and five types of coal were collected and used to
109 generate smoke samples. The biomass materials consisted of three crop straws (wheat straw
110 (WS), rice straw (RS), and corn straw (CS)) and three wood branches (pine wood (PW),
111 Chinese fir (CF), and white poplar (WP)). These materials are usually used as fuels for heating
112 and cooking in rural areas and are also occasionally burned in the field (Fan et al., 2018; Kumar
113 et al., 2018b). The combustion of these crop straws and woody fuels is reported to make a
114 significant contribution to the atmospheric aerosol in China (Shen et al., 2013). The five types

https://doi.org/10.5194/acp-2021-159
Preprint. Discussion started: 23 February 2021


Atmospheric Chemistry and Physics Discussions

of coal were used for the collection of CC-smoke samples. They consisted of four types of bituminous coal (B-1, B-2, B-3, and B-4) and one anthracite coal (AN), representing the major types of coal used for residential CC in China. The details of these samples are provided in the supporting information (SI).

Samples of the smoke emitted from BB and CC were collected in a combustion and sampling system. The system consisted of a combustion hood, clean background air dilution and injection ports, smoke pipe, mixing fan, mixing chamber, $PM_{2.5}$ sampler (JCH-120F, Juchuang Environmental Protection Group Co., Ltd., Shandong, China), and an exhaust port. The details of the sampling procedure are described in our previous study (Fan et al., 2018; Li et al., 2018) and the SI file.

Blank quartz filters were collected before each group of combustion experiments prior to the fuels being ignited. The blank filters were used to correct the mass of smoke as well as the optical signals and DTT consumption by BrC. To prevent the contamination of the following sample, the collection system was cleaned before each new combustion experiment.

### 2.2. Extraction and isolation of BrC fractions

In this study, the WSOC, HULIS, and MSOC fractions were obtained with the solvent extraction method, as described in our previous studies (Fan et al., 2016; Li et al., 2018). Initially, the filter samples were cut into small pieces and ultrasonically extracted three times with 20 mL ultrapure water for 30 min. The extract was filtered through a 0.22 μm polytetrafluoroethylene (PTFE) syringe filter (Jinteng, Tianjin, China), which collected the WSOC fraction. The HULIS fraction in WSOC was further isolated with an SPE (Oasis HLB,

https://doi.org/10.5194/acp-2021-159
Preprint. Discussion started: 23 February 2021


Atmospheric Chemistry and Physics Discussions

200 mg, Waters, Milford, MA, USA) method. The detailed procedure is provided in the SI file.

The MSOC fraction was obtained by a method developed by Cheng et al. (2016) (Cheng et al., 2016). Briefly, a portion of the filter was immersed in methanol (Macklin, >99.9%, Shanghai, China) for 2 h and then filtered through a 0.22 μm PTFE syringe filter. Static digestion without ultrasonic treatment can avoid the loss of PM and facilitate the determination of the dissolved organic matter (DOM) content. Finally, the residual filters were dried in a vacuum dryer. The OC content of MSOC was obtained by subtracting the OC concentration of the extracted filters from untreated filters.

### 2.3. UV-visible spectroscopy

The UV-visible absorption spectra of the BrC solutions were analyzed using a UV-vis spectrophotometer (UV-2600, Shimadzu, Kyoto, Japan). The BrC solution was placed in a 0.01 m quartz cuvette and the UV-vis spectra was recorded from 200 to 700 nm at 1 nm intervals. Milli-Q water was used as a blank reference for the WSOC and HULIS solutions, while pure methanol was used as the blank for the MSOC fraction. The corresponding background was used to determine the interference from the instrument and operational blank sample.

To describe the optical properties of BrC fractions, the AAE and $MAE_{365}$ were calculated in this study. The AAE is a measure of the spectral dependence of chromophores in BrC, while the $MAE_{365}$ can indicate the light absorbing capacity of BrC (Fan et al., 2016; Cheng et al., 2016). The detailed calculations are described in the SI file.

### 2.4. Fluorescence EEM spectroscopy and the PARAFAC model

https://doi.org/10.5194/acp-2021-159
Preprint. Discussion started: 23 February 2021


Atmospheric Chemistry and Physics Discussions

159 The EEM fluorescence spectra of BrC fractions were recorded by an F-4600 fluorescence
160 spectrometer (Hitachi, Tokyo, Japan) using a 0.01 m width quartz cuvette, with a 400 V xenon
161 lamp at room temperature and a 2400 nm/min scanning speed. The scanning ranges for
162 excitation ($E_X$) and emission ($E_M$) were 200–400 nm and 290–520 nm, respectively. The slit
163 width and intervals for $E_X$ and $E_M$ were both set to 5 nm. According to the different solvents
164 used for sample extraction (water and methanol), all EEM spectra were divided into two groups
165 for analysis (66 samples for water-soluble WSOC and HULIS, and 33 samples for MSOC).
166 The PARAFAC modeling procedure was conducted in EFC v1.2, which is an application
167 software based on MATLAB that has the function of conversion, correction, cognition,
168 comparison, and calculation for processing the fluorescence spectra (He and Hur, 2015;
169 Murphy et al., 2011; Murphy et al., 2013). The PARAFAC analysis method that was included
170 in the software was consistent with the calculation made by the drEEM toolkit when using
171 MATLAB (Murphy et al., 2010; Murphy et al., 2013). The PARAFAC was computed using
172 two to seven component models, with non-negativity constraints and a residual analysis, and a
173 split half analysis was used to validate the number of fluorescence components. According to
174 the results of the split-half and core consistency analysis, four component models were chosen
175 for both the WSOC and HULIS fractions and the MSOC. The EEM was normalized to the area
176 under the ultrapure water Raman peak ($E_X$ = 350 nm, $E_M$ = 365–430 nm) collected before the
177 measurement of samples to produce corrected fluorescence intensities in Raman units (Lawaetz
178 and Stedmon, 2009). The relative contribution of individual chromophores was estimated by
179 calculating the maximum fluorescence intensities ($F_{max}$: maximum fluorescence intensity of
180 identified fluorescence components, relative content % = $F_{max}/\Sigma F_{max}$) (Matos et al., 2015; Chen

https://doi.org/10.5194/acp-2021-159
Preprint. Discussion started: 23 February 2021


Atmospheric Chemistry and Physics Discussions

et al., 2016).

### 2.5. Proton-NMR spectroscopy

Approximately 5 mg of the BrC fractions (i.e., HULIS, WSOC, and MSOC) derived from BB and CC were dissolved in 500 μL deuterium oxide and then transferred to a 5 mm NMR tube. The $^{1}$H-NMR spectra were obtained at a frequency of 400 MHz using a spectrometer (Avance III 400, Bruker Daltonik GmbH, Bremen, Germany). Data was acquired from 100 scans, with a recycling time of 2 s for a condensed water sample. The length of the proton 90° pulse was 8.87 μs. A 1.0 Hz line-broadening weighting function and baseline correction were applied. The identification of the functional groups in the NMR spectra was based on their chemical shift (δH) relative to that of tetramethylsilane (0 ppm), which was applied as an internal standard (Zou et al., 2020).

### 2.6. Oxidative potential

The OP of BrC emitted from the BB and CC processes (i.e., WSOC, HULIS, and MSOC) was measured by a DTT assay. The experimental procedure was as described in previous studies (Bates et al., 2019; Verma et al., 2012). Briefly: 3 mL of extracted sample solution (MSOC was a mixture of 100 μL sample and 2.9 mL of 18.2 MΩ Milli-Q water, and the corresponding blank was the same solution as that of the water blank) and 3 mL of 1 mM DTT were mixed in a 20 mL brown vial, and then placed in a 37 °C water bath to maintain the samples at a constant temperature. At a specific time interval (0, 5, 10, 15, and 20 min), 1 mL of the well mixed sample was transferred to another 4 mL brown vial, and 1 ml trichloroacetic

https://doi.org/10.5194/acp-2021-159
Preprint. Discussion started: 23 February 2021


Atmospheric Chemistry and Physics Discussions

acid (TCA 1% w/v) was added to stop the reaction. Then, 0.5 mL 5,5'-dithiobis-(2-nitrobenzoic acid) (DTNB, 1 mM) was added to react with the remaining DTT to produce 2-nitro-5-thiobenzoic acid. After 5 min, 1 mL of tris(hydroxymethyl)methyl aminomethane buffer (0.4 mM Tris buffer, pH 8.9 in 4 mM DTPA) was added and the yellow color of TNB was visible in the mixed samples. The absorbance was measured at 412 nm with a UV-vis spectrometer (UV2600, Shimadzu). The DTT, TCA, and DTNB were all configured with 0.1 M phosphate buffer (pH 7.4), containing 1 mM DTPA. and the corresponding filter blank was analyzed to correct the DTT activity of the sample fractions. The DTT consumption rate after subtracting the filter blank and operating blank were determined using the absorbance and normalized by the particulate mass (pmol/min/μg) (Verma et al., 2012; Fan et al., 2018).

## 3. Results and discussion

### 3.1. Abundance of WSOC, HULIS, and MSOC in BB and CC smoke samples

Table 1 summarizes the abundance of BrC fractions, including WSOC, HULIS, and MSOC, in BB and CC smoke $PM_{2.5}$ samples. As shown in Table 1, the average contribution of WSOC to smoke $PM_{2.5}$ was 2.9%–12% and 2.3%–22% for BB and CC, respectively. This result was comparable to the results obtained for smoke samples from the combustion of cherry leaves (16%) and gingko tree leaves (6.0%) (Park et al., 2013), corn straw (5.9%) and pine branch (6.4%) (Fan et al., 2016), residential coals (4%–11%) (Li et al., 2018), and in ambient $PM_{2.5}$ from rural and urban sites (4–13%) (Matos et al., 2015; Qin et al., 2018; Wu et al., 2020). It suggests that both BB and CC can release substantial amounts of water-soluble BrC into atmospheric aerosols. As the hydrophobic fraction of WSOC, the carbon content of HULIS

https://doi.org/10.5194/acp-2021-159
Preprint. Discussion started: 23 February 2021


Atmospheric Chemistry and Physics Discussions

accounted for 1.0%–7.8% and 0.5%–10% of BB and CC smoke $PM_{2.5}$, respectively. These values are comparable to the results obtained for BB smoke (5.9%–15.2%) (Fan et al., 2018; Huo et al., 2018), CC smoke (1.9%–4.8%) (Li et al., 2018), and atmospheric aerosols in Beijing (4.8%–9.4%) (Li et al., 2019), with an average value of 7.2% ± 3.3%, therefore confirming the important contributions made by BB and CC to atmospheric HULIS. As a comparison, the contribution of MSOC to smoke $PM_{2.5}$ was 6.4%–47% and 9.4%–73% for BB and CC, respectively, with both values being much higher than the contributions of the water-soluble fractions (WSOC and HULIS) in the same smoke samples. Similar results have been reported in many previous studies (Li et al., 2018; Cheng et al., 2016), which suggest that there are more organic compounds that could be extracted by methanol in MSOC than in water-soluble WSOC and HULIS, and it could therefore be the best indicator of total BrC. This result also indicated that BB and CC both released large amounts of water-insoluble BrC compounds, including hydrophobic polycyclic aromatic hydrocarbons (PAHs) and nitrogen/sulfur-containing heteroatomic PAHs (Geng et al., 2014; Dong et al., 2021; Huang et al., 2020).

There were some differences observed among the different types of smoke samples. As shown in Figure 1, the average contribution of the WSOC and HULIS fractions to the total carbon (TC) were 22% ± 7.3% and 11% ± 3.8%, respectively, for BB smoke, which were higher than the corresponding values of 19% ± 9.4% and 8.2% ± 4.0% for CC smoke. The contribution of MSOC to OC was 69% ± 19% for BB, which was significantly lower than the value of 97% ± 1.8% for CC. These results indicated that BB generally released the more water-soluble BrC fraction, whereas the more methanol-soluble BrC fraction was contained in the smoke particles emitted from CC. These differences can be explained by the fact that biomass fuels generally

https://doi.org/10.5194/acp-2021-159
Preprint. Discussion started: 23 February 2021


Atmospheric Chemistry and Physics Discussions

247 contained a large amount of biopolymers, such as carbohydrates (cellulose, hemicellulose, etc),
248 and the burning of biomass fuels would produce more highly polar compounds, whereas more
249 relatively hydrophobic components, such as aromatic species, were emitted from CC (Wu et
250 al., 2014; Wu et al., 2021; Huang et al., 2020).
251
252 **3.2 Light absorption**
253 The AAE and $MAE_{365}$ are important optical indicators of the light absorption properties
254 of atmospheric BrC, which were investigated for BB- and CC-derived BrC in this study. As
255 shown in Figures 2a and c, the AAE values of the WSOC and HULIS fractions were 6.1–9.9
256 (mean 7.8 ± 1.6) and 7.2–9.6 (mean 8.5 ± 0.8), respectively, for BB smoke and 8.5–16 (mean
257 13 ± 2.9) and 10–16 (mean 14 ± 2.3), respectively, for CC smoke. These results were
258 comparable to those measured for combustion emitted aerosols, with reported AAE values for
259 HULIS of 7.4–8.3 (Park and Yu, 2016) and 6.2–8.1 (Fan et al., 2018; Fan et al., 2016) for BB
260 smoke, and 7.5–11 and 5.2–14, respectively, for CC smoke (Li et al., 2018). The AAE values
261 of BB- and CC-derived WSOC and HULIS were comparable to those reported for WSOC in
262 urban aerosol in Beijing (average 7.28 ± 0.24) (Cheng et al., 2016), HULIS in Amazon BB
263 aerosol (~7.10) (Hoffer et al., 2006), the biomass contribution to urban aerosol in Beijing (5.3–
264 5.8) (Yan et al., 2015), and Tibetan Plateau aerosol (7.14–9.35) (Wu et al., 2020), but higher
265 than that (1.2–5.4, mean of 3.2) of water-soluble BrC in Los Angeles (Zhang et al., 2013). The
266 AAE values for MSOC were 5.62–6.95 for BB smoke and 8.46–10.0 for CC smoke. It was
267 obvious that the AAE value of BB MSOC was comparable to that of urban aerosol (average
268 7.10 ± 0.45) in Beijing (Cheng et al., 2016) and the reported value (5.0–6.5) for urban aerosol

https://doi.org/10.5194/acp-2021-159
Preprint. Discussion started: 23 February 2021


Atmospheric Chemistry and Physics Discussions

in India (Mukherjee et al., 2020), but the AAE values of CC MSOC were likely higher than those for urban aerosols.

As shown in Figures 2a and c, the average AAE values of the WSOC, HULIS, and MSOC fractions in BB smokes were all lower than for the same BrC fraction in CC smoke, indicating that BB-derived BrC had a weaker wavelength dependence than CC-derived BrC. This finding agreed with the results reported in a previous study (Fan et al., 2016). The AAE values of the BrC fraction varied according to the type of BrC fraction. HULIS had the highest AAE values, which were slightly higher than those of WSOC but much higher than those of MSOC (Figures 2a and c), indicating that water-soluble BrC fractions had a greater wavelength dependency than the corresponding MSOC. This was similar to the results of previous studies that found higher AAE values for WSOC than MSOC in ambient aerosols (Cheng et al., 2016; Kim et al., 2016) and can be explained by the fact that the strongly light-absorbing organic molecules are generally comprised of aromatic structures, with a high degree of conjugation and low solubility in water.

The $MAE_{365}$ is an important parameter that characterizes the light absorbing ability of atmospheric BrC. As shown in Figures 2b and d, the $MAE_{365}$ values of WSOC and HULIS were 0.9–1.5 (mean 1.2 ± 0.3) and 1.1–1.6 (mean 1.3 ± 0.2) $m^2/gC$, respectively, for BB smoke and 0.2–0.8 (mean 0.3 ± 0.2) and 0.3–1.1 (mean 0.4 ± 0.3) $m^2/gC$, respectively, for CC smoke. As the hydrophobic fraction of WSOC, the $MAE_{365}$ value of HULIS in BB and CC smoke was slightly higher than that of the corresponding WSOC, suggesting that HULIS had a stronger light absorbing ability. Moreover, the $MAE_{365}$ value of WSOC and HULIS in BB smoke was comparable with the results of previous studies of the WSOC and HULIS fractions in

https://doi.org/10.5194/acp-2021-159
Preprint. Discussion started: 23 February 2021


Atmospheric Chemistry and Physics Discussions

combustion derived smoke particulate and ambient aerosols. For example, the reported $MAE_{365}$ values of WSOC and HULIS were 0.8–1.6 and 1.0–1.5 $m^2/gC$, respectively, in BB smoke $PM_{2.5}$ (Park and Yu, 2016; Huo et al., 2018), 0.3–1.0 and 0.5–1.4 $m^2/gC$, respectively, in CC smoke particles (Li et al., 2018), and 0.1–1.5 $m^2/gC$ in ambient aerosols (Cheng et al., 2016; Yan et al., 2015; Zou et al., 2020). In contrast, the $MAE_{365}$ values for MSOC were 1.9–2.7 $m^2/gC$ for BB smoke and 1.0–2.7 $m^2/gC$ for CC smoke, which were 1.3–8.5 times higher than the corresponding values for HULIS and WSOC. These results suggest that MSOC had the strongest light absorption capacity. The $MAE_{365}$ values of primary BB and CC smoke were comparable to the $MAE_{365}$ value of urban aerosol in Beijing winter time (average 1.45 ± 0.26 $m^2/gC$) (Yan et al., 2015), and the water-insoluble BrC (0.85–2.45 $m^2/gC$) in summer and winter ambient aerosol in Xi'an, northwest China (Li et al., 2020b). However, the values were higher than the $MAE_{365}$ value of aerosol MSOC in the Central Tibetan Plateau (0.27–0.86 $m^2/gC$) (Wu et al., 2020), which may be due to the relatively low combustion source contribution in this region.

As shown in Figures 2b and d, some differences were observed among the BrC fractions. WSOC, HULIS, and MSOC in BB smoke all had relatively higher $MAE_{365}$ values than the same BrC fractions from CC, which suggested that BrC components emitted from BB had a relatively higher light absorption ability than those from CC, and may therefore have a higher radiative force (Alexander et al., 2008). In addition, water-soluble BrC from the combustion of the highly mature bituminous coal generally had a relatively higher $MAE_{365}$ value, indicating that it possessed the strongest light absorbing capacity.

https://doi.org/10.5194/acp-2021-159
Preprint. Discussion started: 23 February 2021


Atmospheric Chemistry and Physics Discussions

### 3.3. Spectral EEM features and identification of PARAFAC components

#### 3.3.1. The EEM fluorescence properties

Fluorescence spectroscopy is a highly sensitive analytical technique for the identification of the sources and types of fluorophores in natural organic matter. In recent decades, it has been widely used to characterize the fluorophores of atmospheric BrC in field and laboratory studies (Chen et al., 2017; Chen et al., 2016; Qin et al., 2018; Fan et al., 2020). The typical EEM spectra of WSOC, HULIS, and MSOC fractions from BB and CC are shown in Figure S2. To avoid concentration effects, the fluorescence spectra were normalized by the OC content of WSOC, HULIS, and MSOC, and the specific fluorescence intensities (a.u.L/(gC)) are shown.

In general, the different regions in the fluorescence spectra can be associated with organic fractions with different chemical characteristics (Table S1) (Chen et al., 2003; Cui et al., 2016; Qin et al., 2018). As shown in Figure S2, the EEM spectra were divided into five regions: protein-like amino acid (I), protein-like UV region (II, peak $T_1$), fulvic-like (III), tryptophan-like or microbial byproducts (IV, peak $T_2$), and humic-like (V) fluorophores (Qin et al., 2018; Cui et al., 2016; Chen et al., 2016) It was observed that the WSOC and HULIS fractions exhibited two types of fluorescence peak at $\lambda_{ex}/\lambda_{em} \approx$ (220–240)/(350–390) nm (peak $T_1$) and $\lambda_{ex}/\lambda_{em} \approx$ (260–300)/(240–380) nm (peak $T_2$) (as marked in Figure S2), which were mainly located in regions II and IV, respectively. These bands in the same range as peaks $T_1$ and $T_2$ have previously been identified in the EEM fluorescence spectra of water-soluble organic matter from rainwater/fog water (Santos et al., 2009; Santos et al., 2012), and $PM_{2.5}$ in an industrial city in northwest China (Qin et al., 2018). As shown in Figure S2, the fluorescence peaks $T_1$ and/or $T_2$ were the dominant peaks for WSOC and HULIS in all BB and CC derived

https://doi.org/10.5194/acp-2021-159
Preprint. Discussion started: 23 February 2021


Atmospheric Chemistry and Physics Discussions

smoke samples, which was consistent with previous observations of the WSOC and HULIS fractions from BB (Huo et al., 2018; Fan et al., 2020). In general, the peak $T_1$ mainly corresponded to the protein-like UV region, with a minor contribution from the fulvic-like substances, whereas peak $T_2$ was assigned as tryptophan-like or microbial byproduct fluorophores. However, as reported in recent studies, non-nitrogen-containing species, such as naphthalene and phenol-derived compounds, have a fluorescence similar to the tryptophan-like matter component, which may account for a major portion of the chromophores of peak $T_2$ in atmospheric aerosols (Chen et al., 2017, 2020). In addition, unlike the fluorophores of organic matter in atmospheric environments, the intensity of peak $T_1$ was clearly stronger than the peak in ambient HULIS described in previous studies (Chen et al., 2017; Chen et al., 2016; Fan et al., 2020; Qin et al., 2018), indicating that these BB and CC derived HULIS fractions might consist of more protein-like and/or aromatic amino acids than atmospheric HULIS.

As shown in Figure S2, the EEM spectra of the three MSOC fractions from crop straw burning all had a strong fluorescence peak at long emission wavelengths ($E_X$ = 205–280 nm, $E_M$ = 360–380 nm), which was located in regions V and IV and was generally assigned to humic-like fluorophores (Qin et al., 2018) or less oxygenated humic-like species (Chen et al., 2017; Chen et al., 2016). This peak was very weak or unobservable in the EEM fluorescence spectra of the WSOC and HULIS fractions, suggesting that the higher intensity of the fluorescence peak was mainly due to water-insoluble organic compounds, with a high degree of conjugation and/or aromaticity. As shown in Figure S2, unlike the EEM spectra of crop straw MSOC, the EEM spectra of the three wood branches all displayed two obvious fluorescence peaks (e.g., peaks $T_1$ and $T_2$). These differences in the EEM spectra between crop straw and

https://doi.org/10.5194/acp-2021-159
Preprint. Discussion started: 23 February 2021


Atmospheric Chemistry and Physics Discussions

wood burning-derived MSOC might be attributed to their molecular differences, which should be investigated in future studies. The EEM spectra of the four bituminous coal smoke MSOC fractions displayed a similar fluorescence peak $T_2$ in the EEM spectra, but only a strong peak $T_1$ was observed in the anthracite coal smoke MSOC. These differences indicate that the fluorophores of MSOC were significantly influenced by the type of fuel material.

### 3.3.2. Identification of PARAFAC components

The PARAFAC analysis further determined the fluorescent components of the water-soluble BrC fraction (WSOC and HULIS) and MSOC. As shown in Figure 3a, WSOC and HULIS generally contained four type of fluorophores ($C_W1$–$C_W4$). Based on previous studies of BrC EEM in combustion aerosols and ambient aerosols (Chen et al., 2017; Chen et al., 2016; Huo et al., 2018; Qin et al., 2018), these four fluorophores could be assigned to two protein-like substances ($C_W1$ and $C_W2$), one polyphenol-like component ($C_W3$), and one humic-like compound ($C_W4$). The Ex/Em maximum of $C_W1$ was located at 230/365 nm in region II, and was confirmed to be protein-like UV fluorophores. $C_W2$ ($E_X$ = 270 nm, $E_M$ = 350 nm) was placed in region IV, and was assigned as tryptophan-like or microbial byproduct compounds (Chen et al., 2016; Li et al., 2020a), which have been identified in aerosol WSOM (Chen et al., 2016; Matos et al., 2015) and BB-derived primary and secondary WSOM (Huo et al., 2018). $C_W3$ ($E_X$ = 205/275 nm, $E_M$ = 330 nm) was located in regions I and IV, and had the characteristics of aromatic protein-like fluorophores or polyphenol-like components, most likely represented the fluorescence properties of polyphenol-like components or compounds containing the phenoxy group (Mostofa et al., 2011). $C_W4$ ($E_X$ = 215–320 nm, $E_M$ = 415 nm)

https://doi.org/10.5194/acp-2021-159
Preprint. Discussion started: 23 February 2021


Atmospheric Chemistry and Physics Discussions

was located in the area where regions III and V overlap. These overlapping peaks were assigned to a strong humic-like species fluorescence, with an excitation wavelength = 245 nm, and two weaker shoulder peaks (Chen et al., 2016; Li et al., 2020a; Qin et al., 2018; Huo et al., 2018; Fan et al., 2020); therefore, $C_W4$ was associated with typical humic like fluorophores. In summary, the fluorescence components identified in the WSOC and HULIS fractions suggested that protein-like and humic-like substances were the two major backbone components in the water soluble BrC fractions.

As shown in Figure 3b, four independent fluorescence components were also identified by the PARAFAC analysis of MSOC ($C_M1$–$C_M4$). These components were similar to those of WSOC and HULIS, especially the positioning of the main peaks of the four fluorescent fluorophores. However, some small differences for component 2 ($C_W2$ and $C_M2$) and component 4 ($C_W4$ and $C_M4$) fluorophores were also observed. Unlike $C_W2$ in WSOC and HULIS, $C_M2$ in MSOC had its Ex/Em maximum at 285/360 nm, which was assigned to tryptophan-like compounds (Fan et al., 2020; Qin et al., 2018). In addition, two lower intensity of peaks at a lower excitation wavelength were also detected. The position of this fluorescence was closer to that of the typical tryptophan-like chromophores in aquatic DOM (Murphy et al., 2010). $C_M4$ in MSOC had a strong peak (EX = 255 nm, EM = 295 nm), but without the shoulder peaks observed for $C_W4$ in WSOC (Chen et al., 2016; Hou et al., 2018).

The relative contribution of individual chromophores identified by the PARAFAC analysis were calculated to express the relative contribution of each independent chromophore to the overall fluorescence properties and are shown in Figure 4. The protein-like fluorescence group (components 1 and 2), which were located at low emission wavelengths, dominated the

https://doi.org/10.5194/acp-2021-159
Preprint. Discussion started: 23 February 2021


Atmospheric Chemistry and Physics Discussions

fluorophores of the BrC fractions in most BB and CC smoke samples. As shown in Figure 4, the contributions of protein-like substances in WSOC, HULIS, and MSOC were 47%–80%, 44%–87%, and 42%–70% (except CS MSOC), respectively, which were higher than the contributions of the polyphenol-like or humic-like substances in the same BrC fraction. These results are similar to the results reported for BrC from biomass combustion emissions in previous studies (Huo et al., 2018; Fan et al., 2020). However, they were significantly different from the EEM-PARAFAC properties of BrC in ambient aerosol, in which component 4 was the most abundant chromophore (Chen et al., 2016; Li et al., 2020a). However, component 4 only accounted for 13%–33% (except CS MSOC) and 3.8%–31% of the BB and CC BrC fluorescent intensity, respectively, which was significantly lower than that reported previously in ambient aerosol (30%–38%) (Li et al., 2020a). Moreover the contribution of polyphenol-like chromophores was 4.0%–39% and was comparable to that of ambient aerosol (18%–26%) (Li et al., 2020a; Chen et al., 2016). The four main fluorescent components were all detected in the BrC fractions in combustion-derived smoke and atmospheric aerosols; however, the relative contents of protein-like and humic-like fluorophores were different. The protein-like compounds were the dominant fluorophores in combustion-derived BrC, whereas a relatively higher content of humic-like fluorophores was identified in ambient aerosol BrC. These differences may be due to the influence of various atmospheric chemical processes on the fluorophores (Li et al., 2020a; Fan et al., 2020).

Furthermore, some differences were also observed among the BrC fraction derived from different sources. As shown in Figure 4, the water-soluble BrC (WSOC and HULIS) from wood burning had a relatively higher content of component 3 than the water-soluble BrC from crop

https://doi.org/10.5194/acp-2021-159
Preprint. Discussion started: 23 February 2021


Atmospheric Chemistry and Physics Discussions

straw burning, which may be associated with the relatively large amount of lignin components in wood materials. Moreover, the relative content of protein-like fluorescent groups in MSOC produced by wood burning were slightly higher than in crop straw combustion-derived MSOC. In addition, even though their maturity was very different, there was no regular trend in the relative content of the fluorescent groups.

### 3.4. $^{1}$H-NMR spectroscopy

$^{1}$H-NMR is an important analytical tool for the investigation of the functional groups of WSOC and HULIS in rural/urban aerosol (Fan et al., 2016; Zou et al., 2020) and rainwater (Santos et al., 2009; Santos et al., 2012). The typical $^{1}$H-NMR spectra of the WSOC, HULIS, and MSOC fractions in smoke emitted from BB crop straw (e.g., WS), and CC (e.g., B-1) are shown in Figure 5 and the $^{1}$H-NMR spectra of other BB and CC BrC fractions are shown in Figure S3. These BrC fractions had similar $^{1}$H-NMR spectra to those derived from atmospheric HULIS and/or WSOC in rainwater (Santos et al., 2009; Santos et al., 2012), BB aerosols (Fan et al., 2016), and ambient aerosols in urban and rural regions (Zou et al., 2020).

As shown in Figure 5, the $^{1}$H-NMR spectra were mainly composed of several distinct sharp peaks superimposed on an unresolved broad band. According to previous studies and reference NMR spectra (Zou et al., 2020; Chalbot et al., 2014; Chalbot et al., 2016), these sharp peaks can be ascribed to low molecular weight organic compounds, such as levoglucosan (δ3.52, δ3.67, δ4.08, and δ5.45 ppm), glucose (δ3.88–δ3.91 and δ3.81–δ3.85 ppm), and fructose (δ3.79–δ3.84 ppm) associated with BB emissions; phthalic acid (δ7.45–δ7.47 and δ7.58 ppm) and terephthalic acid (δ8.01 ppm) associated with anthropogenic activity; and the

https://doi.org/10.5194/acp-2021-159
Preprint. Discussion started: 23 February 2021


Atmospheric Chemistry and Physics Discussions

445 $CH_3$ in trimethylamine (δ2.71 and δ2.89 ppm), dimethylamine (δ2.72 ppm), and
446 monomethylamine (δ2.55 ppm) co-emitted with ammonia. The relatively few and/or weak
447 sharp peaks in the $^1$H-NMR spectra of HULIS compared with those of WSOC may be the result
448 of low molecular weight organic compounds that have been removed from HULIS through
449 SPE isolation. In addition, all BB-derived WSOC had a high intensity of sharp peaks associated
450 with carbohydrates, such as levoglucosan, glucose, and fructose resonances, which may be
451 released from the thermal reactions of biopolymers, such as celluloses. As a comparison,
452 several peaks (δ0.90 and δ1.35 ppm) were observed in MSOC, and were mainly located in the
453 aliphatic region. These peaks were weaker in WSOC and HULIS, suggesting more less-polar
454 aliphatic compounds were present in the MSOC fraction.

455 Despite some sharp peaks being identified, most of the signals in the $^1$H-NMR spectra of
456 the BrC fractions were presented as a continuous unresolved distribution, suggesting that BrC
457 consists of a complex mixture of organic substances (Fan et al., 2016; Chalbot et al., 2014;
458 Chalbot et al., 2016). As shown in Figure 5, the functional groups of smoke BrC could be
459 divided into four representative categories: (1) R-H: aliphatic protons in alkyl chains (0.6–1.9
460 ppm), including the methyl (R-$CH_3$) proton, methylene (R-$CH_2$) proton, and methyne (R-CH)
461 proton; (2) H-C-C=: aliphatic protons bound to carbon atoms adjacent to unsaturated groups
462 (1.9–3.2 ppm), including carbonyl (H-C-C=O) and imino (H-C-C=N) groups or aromatic rings;
463 (3) H-C-O: protons bound to oxygenated aliphatic carbons atoms in alcohols, polyols, ethers,
464 and esters (3.4–4.4 ppm), generally indicating that carbohydrates and ethers were present in
465 organic matter; and (4) Ar-H: protons bound to aromatic carbon atoms (6.5–8.5 ppm) (Fan et
466 al., 2016; Zou et al., 2020).

https://doi.org/10.5194/acp-2021-159
Preprint. Discussion started: 23 February 2021


Atmospheric Chemistry and Physics Discussions

Table 2 shows the distribution of the four types of protons described above, which was obtained by integrating the area of the observed $^{1}$H-NMR bands for each sample. The four types of proton groups (e.g., R-H, H-C-C=, H-C-O, and Ar-H) were all identified in the $^{1}$H-NMR spectra of the BB and CC derived BrC fractions, but the relative distribution of these four functional groups were different. The four functional groups have been observed in the $^{1}$H-NMR spectra of WSOC and HULIS in ambient aerosols, but again the relative distribution of the four functional groups were different. In general, HULIS in ambient aerosols (Chalbot et al., 2014; Chalbot et al., 2016) and rainwater (Santos et al., 2012) were all characterized by the predominance of H-C (41%–60%), moderate contents of H-C-C= (25%–34%) and H-C-O (4.0%–49%), and a lesser contribution of Ar-H (2.0%–6.0%). However, it was obvious that the relative content of Ar–H groups (18%–37%) in HULIS from both combustion processes (BB and CC) was higher than the levels in ambient HULIS (Table 2), which suggests that BB and CC derived HULIS contained more aromatic structures than ambient HULIS. This was consistent with reports that more aromatic structures are observed in HULIS in colder season aerosol particles in northern China, which may be related to the amount of residential coal and straw combustion (Li et al., 2018; Sun et al., 2017).

As shown in Table 2, the relative contents of the four functional groups varied with the type of BrC. For example, BB WSOC was always characterized by a relatively high level of oxygenated H-C-O groups and relatively low level of aliphatic R-H groups compared with the corresponding MSOC extracted with methanol. As shown in Figure 5, several strong signals in aliphatic R-H were identified in MSOC, but they were weaker in the WSOC fraction. The oxygenated aliphatic compounds (generally assigned as polyols or polysaccharides) produced

https://doi.org/10.5194/acp-2021-159
Preprint. Discussion started: 23 February 2021


Atmospheric Chemistry and Physics Discussions

489 higher signals in the WSOC fraction, especially those from BB. This was considered reasonable
490 because the less-polar aliphatic compounds were difficult to dissolve in water but could be
491 extracted by methanol. As the hydrophobic fraction of WSOC, HULIS contained a relatively
492 higher content of the Ar-H group and relatively lower content of the oxygenated H-C-O group
493 than the original WSOC for all BB and CC smoke samples. This was due to most of the low
494 molecular oxygenated compounds not being retained by the hydrophilic-lipophilic balance
495 cartridges and the enrichment of aromatic species (Fan et al., 2016; Zou et al., 2020).

496 Although there were similarities among the BrC fractions formed from the combustion of
497 biomass materials and coal, some distinct differences in the distribution of functional groups
498 were also observed. As shown in Figure 5, several oxygenated compounds (e.g., levoglucosan)
499 were identified, with higher intensity signals in the WSOC fractions of BB smoke particles, but
500 they were weaker than the WSOC fractions of CC smoke particles. The relative content of the
501 H-C-O group was in the range of 34%–54% for the six BB WSOC, which was higher than the
502 9.0–34% value for the five CC WSOC. These oxygenated aliphatic compounds were mainly
503 assigned to carbohydrate and polyols that may be caused by the degradation of BB-derived
504 from lignin substances (Fan et al., 2012; Fan et al., 2016; Lin et al., 2016). Therefore, these
505 differences could be ascribed to the fact that the HULIS from BB contained a relatively high
506 content of carbohydrate derived compounds. In contrast, the BrC fractions from CC indicated
507 a relatively higher level of unsaturated functional groups compared with the BrC fractions from
508 BB (Table 2). For example, there was a relatively higher content of Ar–H (30%–37%) and H-
509 C-C= (34%–40%) in the smoke HULIS from CC than from BB, indicating that residential CC
510 emitted HULIS contained more aromatic structures and unsaturated aliphatics, e.g., PAHs (Wu

https://doi.org/10.5194/acp-2021-159
Preprint. Discussion started: 23 February 2021


Atmospheric Chemistry and Physics Discussions

et al., 2014; Dong et al., 2021; Huang et al., 2020).

Furthermore, some differences were also identified between the BrC fractions from the burning of crops and wood. As shown in Table 2, relatively higher contents of the H-C-O group were found in the BrC fractions in smoke particles from wood burning, whereas relatively higher contents of the R-H group were found in the BrC fractions in smoke particles from crop burning. For example, the content of the H-C-O group in wood WSOC was in the range of 48%–54%, which was slightly higher than the 34%–46% value for crop straw WSOC. These results were inconsistent with the levels of carbohydrate components reported in grass, which suggests that the chemical composition of BrC is also influenced by the combustion temperature (Atwi et al., 2021).

### 3.5 Oxidative potential

The OP of the BB and CC derived BrC fractions (i.e., WSOC, HULIS, and MSOC) were investigated through a DTT assay and the results are shown in Table S2 and Figure 6. The $DTT_{mass}$ value of WSOC ranged from 0.5 pmol/min/μg (B-3) to 7.37 pmol/min/μg (CS), with a mean of 3.8 pmol/min/μg. These $DTT_{mass}$ values were much lower than the range of 12.5–20.6 pmol/min/μg reported for wood burning aerosol and 14–25 pmol/min/μg in Los Angeles wildfire samples (Bates et al., 2019; Fan et al., 2018), as well as the range of 22−68 pmol/min/μg reported for water extracts from atmospheric particles (Verma et al., 2012). These results suggested that the primary smoke from BB and CC in this study had a weaker ROS generation capacity than ambient aerosols, which was likely due to the differences in the chemical composition of WSOC in BB and CC smoke particles and ambient aerosols (Lin and

https://doi.org/10.5194/acp-2021-159
Preprint. Discussion started: 23 February 2021


Atmospheric Chemistry and Physics Discussions

Yu, 2011; Dou et al., 2015; Wong et al., 2019; Lin and Yu, 2019). For example, ambient aerosols (e.g., vehicle emissions) generally contain many redox compounds, which may contribute more transition metals and quinones (Ma et al., 2018; Lin and Yu, 2011).

The $DTT_{mass}$ values of BB and CC derived HULIS ranged from 0.5 pmol/min/μg (B-3) to 5.5 pmol/min/μg (RS), with a mean of 2.3 pmol/min/μg. These values were lower than the range (15–45 pmol/min/μg) previously reported for ambient HULIS, also measured with the same DTT assay (Lin and Yu, 2011; Ma et al., 2018; Verma et al., 2012). In addition, HULIS accounted for a wide range (41.4%–90.6%) of the DTT activity in WSOC in the BB and CC samples, indicating that the hydrophobic fractions were important redox-active compounds in the BB and CC derived WSOC fractions. Similar results were obtained for the oxidative contribution of HULIS following water extracts from ambient aerosols in many previous studies (Ma et al., 2018; Lin and Yu, 2019; Lin and Yu, 2011).

The $DTT_{mass}$ values of MSOC were in the range of 3.1 pmol/min/μg (B-4) to 84 pmol/min/μg (RS). These values were comparable to those reported in previous studies involving atmospheric aerosol methanol extracts (~55 pmol/min/μg) (Verma et al., 2012). As shown in Figure 6, the $DTT_{mass}$ values of MSOC were much higher than those of WSOC and HULIS from the same smoke samples, which suggested that the water-insoluble components possessed significant oxidative properties that are relevant in toxicological studies (Verma et al., 2012). These results were consistent with the results of previous studies that water-insoluble compounds made the largest contribution to the OP (Verma et al., 2012; Verma et al., 2015).

The $DTT_{mass}$ values of the BrC fractions varied with the type of fuel material. As shown in Table S2, the $DTT_{mass}$ values of BB WSOC were 4.5–7.4 pmol/min/μg, which was

https://doi.org/10.5194/acp-2021-159
Preprint. Discussion started: 23 February 2021


Atmospheric Chemistry and Physics Discussions

555 significantly higher than the range of 0.5–2.1 pmol/min/μg for CC WSOC. Similar results were
556 also observed for the HULIS and MSOC fractions (Figure 6). These results indicated that the
557 BrC fractions from BB had higher OP values than those from CC, and therefore more readily
558 catalyzed the generation of ROS. Furthermore, no regular variations were observed for the OP
559 of water-soluble BrC (e.g., WSOC and HULIS) in BB or CC smoke samples, but the MSOC
560 in crop straw smoke had a much higher $DTT_{mass}$ value than the MSOC in smoke samples from
561 wood burning and CC. These differences were associated with the differences in the amount of
562 redox-active compounds in each BrC fraction. There is a need for more studies to investigate
563 the relationship between the molecular structures in BB smoke BrC and their DTT activities.
564
565 **4. Conclusions**
566 In this study, the primary BrC fractions (i.e., WSOC, HULIS, and MSOC) emitted from
567 BB and CC were comprehensively investigated to determine their content, light absorption,
568 fluorophores, chemical properties, and OP. The results indicated that both BB and CC were
569 important sources of atmospheric BrC. It was found that BB generated more of the water-
570 soluble BrC fraction, whereas CC released more of the methanol-soluble BrC fraction in smoke
571 $PM_{2.5}$. The results also enhanced our understanding of the optical characteristics, chemical
572 composition, and OP of the water and methanol soluble BrC fractions. The MSOC fraction had
573 higher $MAE_{365}$ values than HULIS and WSOC, suggesting that water-insoluble BrC possessed
574 a stronger light absorbing capacity. In addition, BB BrC generally had higher $MAE_{365}$ and
575 lower AAE values than the corresponding CC BrC fractions, suggesting that the former had a
576 higher light absorption ability and weaker wavelength dependence. The EEM-PARAFAC

https://doi.org/10.5194/acp-2021-159
Preprint. Discussion started: 23 February 2021


Atmospheric Chemistry and Physics Discussions

577 analysis identified two protein-like compounds, one polyphenol-like component, and one
578 humic-like compound for all BrC fractions, in which the protein-like compounds were the
579 dominant components. The $^{1}$H NMR analysis showed that the BB and CC BrC fractions
580 contained R-H, H-C-C=, H-C-O, and Ar-H groups, in which WSOC and HULIS were always
581 characterized by more oxygenated H-C-O groups and fewer aliphatic R-H groups than MSOC.
582 In addition, water soluble BB BrC contained more of the highly oxygenated groups, suggesting
583 that they may have a stronger influence on the binding of metals by organic aerosols. Our study
584 also indicated that MSOC had higher $DTT_{mass}$ values than WSOC and HULIS, suggesting a
585 higher ROS generation capacity. The BB BrC fractions generally had a higher OP than CC BrC,
586 which may suggest that BB BrC were more readily able to catalyze the generation of ROS, and
587 therefore lead to more severe harm to human health.
588 It should be noted that the BB and CC BrC fractions would experience a series of chemical
589 reactions once they are emitted into the atmosphere, resulting in changes to their optical
590 properties and OP. Thus, future studies should focus on the chemical, optical, and OP
591 characteristics of BrC during the aging processes with smoke particles in the tropospheric
592 environment (Fan et al., 2020; Wong et al., 2019).
593
594 **Data availability.** The research data can be accessed on request to the corresponding author
595 (songjzh@gig.ac.cn).
596
597 **Author contributions.** J. Song and P. Peng designed the research together. T. Cao, M. Li, and
598 C. Zou carried out the combustion experiments. T. Cao, M. Li, and C Yu extracted and analyzed

https://doi.org/10.5194/acp-2021-159
Preprint. Discussion started: 23 February 2021




BrC fractions. T. Cao and J. Song wrote the paper. X. Fan, J Wang, Z Yu, and P. Peng commented and revised the paper.

**Competing interests.** The authors declare that they have no conflict of interest.

**Acknowledgments.** This study was supported by the National Natural Science Foundation of China (41977188, 41673177), State Key Laboratory of Organic Geochemistry, GIGCAS (SKLOG2020-3), Guangdong Foundation for Program of Science and Technology Research (2019B121205006).

## References

Alexander, D. T. L., Crozier, P. A., and Anderson, J. R.: Brown carbon spheres in East Asian outflow and their optical properties, Science, 321, 833-836, 10.1126/science.1155296, 2008.

Andreae, M. O., and Gelencser, A.: Black carbon or brown carbon? The nature of light-absorbing carbonaceous aerosols, Atmospheric Chemistry and Physics, 6, 3131-3148, DOI 10.5194/acp-6-3131-2006, 2006.

Atwi, K., Mondal, A., Pant, J., Cheng, Z., El Hajj, O., Ijeli, I., Handa, H., and Saleh, R.: Physicochemical properties and cytotoxicity of brown carbon produced under different combustion conditions, Atmospheric Environment, 244, 117881, 10.1016/j.atmosenv.2020.117881, 2021.

Bates, J. T., Fang, T., Verma, V., Zeng, L., Weber, R. J., Tolbert, P. E., Abrams, J. Y., Sarnat, S.

https://doi.org/10.5194/acp-2021-159
Preprint. Discussion started: 23 February 2021


Atmospheric Chemistry and Physics Discussions

621 E., Klein, M., Mulholland, J. A., and Russell, A. G.: Review of Acellular Assays of
622 Ambient Particulate Matter Oxidative Potential: Methods and Relationships with
623 Composition, Sources, and Health Effects, Environmental science & technology, 53,
624 4003-4019, 10.1021/acs.est.8b03430, 2019.
625 Chalbot, M. G., Brown, J., Chitranshi, P., da Costa, G. G., Pollock, E. D., and Kavouras, I. G.:
626 Functional characterization of the water-soluble organic carbon of size-fractionated
627 aerosol in the southern Mississippi Valley, Atmos Chem Phys, 14, 6075-6088,
628 10.5194/acp-14-6075-2014, 2014.
629 Chalbot, M. G., Chitranshi, P., da Costa, G. G., Pollock, E., and Kavouras, I. G.:
630 Characterization of water-soluble organic matter in urban aerosol by (1)H-NMR
631 spectroscopy, Atmos Environ (1994), 128, 235-245, 10.1016/j.atmosenv.2015.12.067,
632 2016.
633 Chen, Q., Miyazaki, Y., Kawamura, K., Matsumoto, K., Coburn, S., Volkamer, R., Iwamoto,
634 Y., Kagami, S., Deng, Y., Ogawa, S., Ramasamy, S., Kato, S., Ida, A., Kajii, Y., and
635 Mochida, M.: Characterization of Chromophoric Water-Soluble Organic Matter in Urban,
636 Forest, and Marine Aerosols by HR-ToF-AMS Analysis and Excitation-Emission Matrix
637 Spectroscopy, Environmental science & technology, 50, 10351-10360,
638 10.1021/acs.est.6b01643, 2016.
639 Chen, Q., Ikemori, F., Nakamura, Y., Vodicka, P., Kawamura, K., and Mochida, M.: Structural
640 and Light-Absorption Characteristics of Complex Water-Insoluble Organic Mixtures in
641 Urban Submicrometer Aerosols, Environmental science & technology, 51, 8293-8303,
642 10.1021/acs.est.7b01630, 2017.

https://doi.org/10.5194/acp-2021-159
Preprint. Discussion started: 23 February 2021


Atmospheric Chemistry and Physics Discussions

643 Chen, Q., Wang, M., Wang, Y., Zhang, L., Li, Y., and Han, Y.: Oxidative Potential of Water-
644 Soluble Matter Associated with Chromophoric Substances in PM2.5 over Xi'an, China,
645 Environmental science & technology, 53, 8574-8584, 10.1021/acs.est.9b01976, 2019.
646 Chen, W., Westerhoff, P., Leenheer, J. A., and Booksh, K.: Fluorescence excitation - Emission
647 matrix regional integration to quantify spectra for dissolved organic matter,
648 Environmental science & technology, 37, 5701-5710, 10.1021/es034354c, 2003.
649 Chen, Y., and Bond, T. C.: Light absorption by organic carbon from wood combustion,
650 Atmospheric Chemistry and Physics, 10, 1773-1787, DOI 10.5194/acp-10-1773-2010,
651 2010.
652 Cheng, Y., He, K. B., Du, Z. Y., Engling, G., Liu, J. M., Ma, Y. L., Zheng, M., and Weber, R.
653 J.: The characteristics of brown carbon aerosol during winter in Beijing, Atmospheric
654 Environment, 127, 355-364, 10.1016/j.atmosenv.2015.12.035, 2016.
655 Cui, X., Zhou, D., Fan, W., Huo, M., Crittenden, J. C., Yu, Z., Ju, P., and Wang, Y.: The
656 effectiveness of coagulation for water reclamation from a wastewater treatment plant that
657 has a long hydraulic and sludge retention times: A case study, Chemosphere, 157, 224-
658 231, 10.1016/j.chemosphere.2016.05.009, 2016.
659 Dong, Z., Jiang, N., Zhang, R., Xu, Q., Ying, Q., Li, Q., and Li, S.: Molecular characteristics,
660 source contributions, and exposure risks of polycyclic aromatic hydrocarbons in the core
661 city of Central Plains Economic Region, China: Insights from the variation of haze levels,
662 The Science of the total environment, 757, 143885, 10.1016/j.scitotenv.2020.143885,
663 2021.
664 Dou, J., Lin, P., Kuang, B. Y., and Yu, J. Z.: Reactive Oxygen Species Production Mediated by

https://doi.org/10.5194/acp-2021-159
Preprint. Discussion started: 23 February 2021


Atmospheric Chemistry and Physics Discussions

665 Humic-like Substances in Atmospheric Aerosols: Enhancement Effects by Pyridine,
666 Imidazole, and Their Derivatives, Environmental science & technology, 49, 6457-6465,
667 10.1021/es5059378, 2015.
668 Evangeliou, N., Kylling, A., Eckhardt, S., Myroniuk, V., Stebel, K., Paugam, R., Zibtsev, S.,
669 and Stohl, A.: Open fires in Greenland in summer 2017: transport, deposition and radiative
670 effects of BC, OC and BrC emissions, Atmospheric Chemistry and Physics, 19, 1393-
671 1411, 10.5194/acp-19-1393-2019, 2019.
672 Fan, X., Li, M., Cao, T., Cheng, C., Li, F., Xie, Y., Wei, S., Song, J., and Peng, P. a.: Optical
673 properties and oxidative potential of water-and alkaline-soluble brown carbon in smoke
674 particles emitted from laboratory simulated biomass burning, Atmospheric Environment,
675 194, 48-57, 10.1016/j.atmosenv.2018.09.025, 2018.
676 Fan, X., Cao, T., Yu, X., Wang, Y., Xiao, X., Li, F., Xie, Y., Ji, W., Song, J., Peng, P., amp, apos,
677 and an: The evolutionary behavior of chromophoric brown carbon during ozone aging of
678 fine particles from biomass burning, Atmospheric Chemistry and Physics, 20, 4593-4605,
679 10.5194/acp-20-4593-2020, 2020.
680 Fan, X. J., Song, J. Z., and Peng, P. A.: Comparison of isolation and quantification methods to
681 measure humic-like substances (HULIS) in atmospheric particles, Atmospheric
682 Environment, 60, 366-374, 10.1016/j.atmosenv.2012.06.063, 2012.
683 Fan, X. J., Wei, S. Y., Zhu, M. B., Song, J. Z., and Peng, P. A.: Comprehensive characterization
684 of humic-like substances in smoke PM2.5 emitted from the combustion of biomass
685 materials and fossil fuels, Atmospheric Chemistry and Physics, 16, 13321-13340,
686 10.5194/acp-16-13321-2016, 2016.

https://doi.org/10.5194/acp-2021-159
Preprint. Discussion started: 23 February 2021


Atmospheric Chemistry and Physics Discussions

687 Geng, C., Chen, J., Yang, X., Ren, L., Yin, B., Liu, X., and Bai, Z.: Emission factors of
688 polycyclic aromatic hydrocarbons from domestic coal combustion in China, Journal of
689 environmental sciences, 26, 160-166, 10.1016/s1001-0742(13)60393-9, 2014.
690 He, W., and Hur, J.: Conservative behavior of fluorescence EEM-PARAFAC components in
691 resin fractionation processes and its applicability for characterizing dissolved organic
692 matter, Water research, 83, 217-226, 10.1016/j.watres.2015.06.044, 2015.
693 Hoffer, A., Gelencser, A., Guyon, P., Kiss, G., Schmid, O., Frank, G. P., Artaxo, P., and Andreae,
694 M. O.: Optical properties of humic-like substances (HULIS) in biomass-burning aerosols,
695 Atmospheric Chemistry and Physics, 6, 3563-3570, DOI 10.5194/acp-6-3563-2006, 2006.
696 Hou, C., Shao, L., Hu, W., Zhang, D., Zhao, C., Xing, J., Huang, X., and Hu, M.: Characteristics
697 and aging of traffic-derived particles in a highway tunnel at a coastal city in southern
698 China, The Science of the total environment, 619-620, 1385-1393,
699 10.1016/j.scitotenv.2017.11.165, 2018.
700 Huang, R. J., Yang, L., Shen, J., Yuan, W., Gong, Y., Guo, J., Cao, W., Duan, J., Ni, H., Zhu,
701 C., Dai, W., Li, Y., Chen, Y., Chen, Q., Wu, Y., Zhang, R., Dusek, U., O'Dowd, C., and
702 Hoffmann, T.: Water-Insoluble Organics Dominate Brown Carbon in Wintertime Urban
703 Aerosol of China: Chemical Characteristics and Optical Properties, Environmental
704 science & technology, 54, 7836-7847, 10.1021/acs.est.0c01149, 2020.
705 Huo, Y. Q., Li, M., Jiang, M. H., and Qi, W. M.: Light absorption properties of HULIS in
706 primary particulate matter produced by crop straw combustion under different moisture
707 contents and stacking modes, Atmospheric Environment, 191, 490-499,
708 10.1016/j.atmosenv.2018.08.038, 2018.

https://doi.org/10.5194/acp-2021-159
Preprint. Discussion started: 23 February 2021


Atmospheric Chemistry and Physics Discussions

709 Izhar, S., Gupta, T., and Panday, A. K.: Improved method to apportion optical absorption by
710 black and brown carbon under the influence of haze and fog at Lumbini, Nepal, on the
711 Indo-Gangetic Plains, Environmental pollution, 263, 114640,
712 10.1016/j.envpol.2020.114640, 2020.
713 Kim, H., Kim, J. Y., Jin, H. C., Lee, J. Y., and Lee, S. P.: Seasonal variations in the light-
714 absorbing properties of water-soluble and insoluble organic aerosols in Seoul, Korea,
715 Atmospheric Environment, 129, 234-242, 10.1016/j.atmosenv.2016.01.042, 2016.
716 Kramer, A. J., Rattanavaraha, W., Zhang, Z., Gold, A., Surratt, J. D., and Lin, Y.-H.: Assessing
717 the oxidative potential of isoprene-derived epoxides and secondary organic aerosol,
718 Atmospheric Environment, 130, 211-218, 10.1016/j.atmosenv.2015.10.018, 2016.
719 Kumar, N. K., Corbin, J. C., Bruns, E. A., Massabo, D., Slowik, J. G., Drinovec, L., Mocnik,
720 G., Prati, P., Vlachou, A., Baltensperger, U., Gysel, M., El-Haddad, I., and Prevot, A. S.
721 H.: Production of particulate brown carbon during atmospheric aging of residential wood-
722 burning emissions, Atmospheric Chemistry and Physics, 18, 17843-17861, 10.5194/acp-
723 18-17843-2018, 2018a.
724 Kumar, V., Rajput, P., and Goel, A.: Atmospheric abundance of HULIS during wintertime in
725 Indo-Gangetic Plain: impact of biomass burning emissions, Journal of Atmospheric
726 Chemistry, 75, 385-398, 10.1007/s10874-018-9381-4, 2018b.
727 Laskin, A., Laskin, J., and Nizkorodov, S. A.: Chemistry of atmospheric brown carbon,
728 Chemical reviews, 115, 4335-4382, 10.1021/cr5006167, 2015.
729 Lawaetz, A. J., and Stedmon, C. A.: Fluorescence Intensity Calibration Using the Raman
730 Scatter Peak of Water, Applied Spectroscopy, 63, 936-940,

https://doi.org/10.5194/acp-2021-159
Preprint. Discussion started: 23 February 2021


Atmospheric Chemistry and Physics Discussions

731 10.1366/000370209788964548, 2009.

732 Li, J., Chen, Q., Hua, X., Chang, T., and Wang, Y.: Occurrence and sources of chromophoric
733 organic carbon in fine particulate matter over Xi'an, China, The Science of the total
734 environment, 725, 138290, 10.1016/j.scitotenv.2020.138290, 2020a.

735 Li, J., Zhang, Q., Wang, G., Li, J., Wu, C., Liu, L., Wang, J., Jiang, W., Li, L., Ho, K. F., and
736 Cao, J.: Optical properties and molecular compositions of water-soluble and water-
737 insoluble brown carbon (BrC) aerosols in northwest China, Atmospheric Chemistry and
738 Physics, 20, 4889-4904, 10.5194/acp-20-4889-2020, 2020b.

739 Li, M., Fan, X., Zhu, M., Zou, C., Song, J., Wei, S., Jia, W., and Peng, P.: Abundances and light
740 absorption properties of brown carbon emitted from residential coal combustion in China,
741 Environmental science & technology, 10.1021/acs.est.8b05630, 2018.

742 Li, X., Han, J., Hopke, P. K., Hu, J., Shu, Q., Chang, Q., and Ying, Q.: Quantifying primary
743 and secondary humic-like substances in urban aerosol based on emission source
744 characterization and a source-oriented air quality model, Atmospheric Chemistry and
745 Physics, 19, 2327-2341, 10.5194/acp-19-2327-2019, 2019.

746 Lin, M., and Yu, J. Z.: Dithiothreitol (DTT) concentration effect and its implications on the
747 applicability of DTT assay to evaluate the oxidative potential of atmospheric aerosol
748 samples, Environmental pollution, 251, 938-944, 10.1016/j.envpol.2019.05.074, 2019.

749 Lin, P., and Yu, J. Z.: Generation of reactive oxygen species mediated by humic-like substances
750 in atmospheric aerosols, Environmental science & technology, 45, 10362-10368,
751 10.1021/es2028229, 2011.

752 Lin, P., Laskin, J., Nizkorodov, S. A., and Laskin, A.: Revealing Brown Carbon Chromophores

https://doi.org/10.5194/acp-2021-159
Preprint. Discussion started: 23 February 2021


Atmospheric Chemistry and Physics Discussions

753 Produced in Reactions of Methylglyoxal with Ammonium Sulfate, Environmental science
754 & technology, 49, 14257-14266, 10.1021/acs.est.5b03608, 2015.
755 Lin, P., Aiona, P. K., Li, Y., Shiraiwa, M., Laskin, J., Nizkorodov, S. A., and Laskin, A.:
756 Molecular Characterization of Brown Carbon in Biomass Burning Aerosol Particles,
757 Environmental science & technology, 50, 11815-11824, 10.1021/acs.est.6b03024, 2016.
758 Ma, Y., Cheng, Y., Qiu, X., Cao, G., Fang, Y., Wang, J., Zhu, T., Yu, J., and Hu, D.: Sources
759 and oxidative potential of water-soluble humic-like substances
760 (HULIS<sub>WS</sub>) in fine particulate matter
761 (PM<sub>2.5</sub>) in Beijing, Atmospheric Chemistry and Physics, 18,
762 5607-5617, 10.5194/acp-18-5607-2018, 2018.
763 Matos, J. T. V., Freire, S. M. S. C., Duarte, R. M. B. O., and Duarte, A. C.: Natural organic
764 matter in urban aerosols: Comparison between water and alkaline soluble components
765 using excitation-emission matrix fluorescence spectroscopy and multiway data analysis,
766 Atmospheric Environment, 102, 1-10, 10.1016/j.atmosenv.2014.11.042, 2015.
767 Mostofa, K. M. G., Wu, F. C., Liu, C. Q., Vione, D., Yoshioka, T., Sakugawa, H., and Tanoue,
768 E.: Photochemical, microbial and metal complexation behavior of fluorescent dissolved
769 organic matter in the aquatic environments, Geochem. J., 45, 235-254, 2011.
770 Moufarrej, L., Courcot, D., and Ledoux, F.: Assessment of the PM2.5 oxidative potential in a
771 coastal industrial city in Northern France: Relationships with chemical composition, local
772 emissions and long range sources, The Science of the total environment, 748, 141448,
773 10.1016/j.scitotenv.2020.141448, 2020.
774 Mukherjee, A., Dey, S., Rana, A., Jia, S., Banerjee, S., and Sarkar, S.: Sources and atmospheric

https://doi.org/10.5194/acp-2021-159
Preprint. Discussion started: 23 February 2021


Atmospheric Chemistry and Physics Discussions

775 processing of brown carbon and HULIS in the Indo-Gangetic Plain: Insights from
776 compositional analysis, Environmental pollution, 267, 115440,
777 10.1016/j.envpol.2020.115440, 2020.
778 Murphy, K. R., Butler, K. D., Spencer, R. G. M., Stedmon, C. A., Boehme, J. R., and Aiken, G.
779 R.: Measurement of Dissolved Organic Matter Fluorescence in Aquatic Environments: An
780 Interlaboratory Comparison, Environmental science & technology, 44, 9405-9412,
781 10.1021/es102362t, 2010.
782 Murphy, K. R., Hambly, A., Singh, S., Henderson, R. K., Baker, A., Stuetz, R., and Khan, S. J.:
783 Organic matter fluorescence in municipal water recycling schemes: toward a unified
784 PARAFAC model, Environmental science & technology, 45, 2909-2916,
785 10.1021/es103015e, 2011.
786 Murphy, K. R., Stedmon, C. A., Graeber, D., and Bro, R.: Fluorescence spectroscopy and multi-
787 way techniques. PARAFAC, Analytical Methods, 5, 6557, 10.1039/c3ay41160e, 2013.
788 Nozière, B., González, N. J. D., Borg-Karlson, A.-K., Pei, Y., Redeby, J. P., Krejci, R., Dommen,
789 J., Prevot, A. S. H., and Anthonsen, T.: Atmospheric chemistry in stereo: A new look at
790 secondary organic aerosols from isoprene, Geophysical Research Letters, 38, n/a-n/a,
791 10.1029/2011gl047323, 2011.
792 Park, S.-S., Sim, S. Y., Bae, M.-S., and Schauer, J. J.: Size distribution of water-soluble
793 components in particulate matter emitted from biomass burning, Atmospheric
794 Environment, 73, 62-72, 10.1016/j.atmosenv.2013.03.025, 2013.
795 Park, S. S., and Yu, J.: Chemical and light absorption properties of humic-like substances from
796 biomass burning emissions under controlled combustion experiments, Atmospheric

https://doi.org/10.5194/acp-2021-159
Preprint. Discussion started: 23 February 2021


797 Environment, 136, 114-122, 10.1016/j.atmosenv.2016.04.022, 2016.
798 Qin, J., Zhang, L., Zhou, X., Duan, J., Mu, S., Xiao, K., Hu, J., and Tan, J.: Fluorescence
799 fingerprinting properties for exploring water-soluble organic compounds in PM 2.5 in an
800 industrial city of northwest China, Atmospheric Environment, 184, 203-211,
801 10.1016/j.atmosenv.2018.04.049, 2018.
802 Santos, P. S., Otero, M., Duarte, R. M., and Duarte, A. C.: Spectroscopic characterization of
803 dissolved organic matter isolated from rainwater, Chemosphere, 74, 1053-1061,
804 10.1016/j.chemosphere.2008.10.061, 2009.
805 Santos, P. S., Santos, E. B., and Duarte, A. C.: First spectroscopic study on the structural
806 features of dissolved organic matter isolated from rainwater in different seasons, The
807 Science of the total environment, 426, 172-179, 10.1016/j.scitotenv.2012.03.023, 2012.
808 Shen, G., Chen, Y., Wei, S., Fu, X., Zhu, Y., and Tao, S.: Mass absorption efficiency of
809 elemental carbon for source samples from residential biomass and coal combustions,
810 Atmospheric Environment, 79, 79-84, 10.1016/j.atmosenv.2013.05.082, 2013.
811 Singh, G. K., Choudhary, V., Rajeev, P., Paul, D., and Gupta, T.: Understanding the origin of
812 carbonaceous aerosols during periods of extensive biomass burning in northern India,
813 Environmental pollution, 270, 116082, 10.1016/j.envpol.2020.116082, 2021.
814 Sun, J., Zhi, G., Hitzenberger, R., Chen, Y., Tian, C., Zhang, Y., Feng, Y., Cheng, M., Zhang,
815 Y., Cai, J., Chen, F., Qiu, Y., Jiang, Z., Li, J., Zhang, G., and Mo, Y.: Emission factors and
816 light absorption properties of brown carbon from household coal combustion in China,
817 Atmospheric Chemistry and Physics, 17, 4769-4780, 10.5194/acp-17-4769-2017, 2017.
818 van der Werf, G. R., Randerson, J. T., Giglio, L., Collatz, G. J., Mu, M., Kasibhatla, P. S.,

https://doi.org/10.5194/acp-2021-159
Preprint. Discussion started: 23 February 2021




819 Morton, D. C., DeFries, R. S., Jin, Y., and van Leeuwen, T. T.: Global fire emissions and
820 the contribution of deforestation, savanna, forest, agricultural, and peat fires (1997-2009),
821 Atmospheric Chemistry and Physics, 10, 11707-11735, 10.5194/acp-10-11707-2010,
822 2010.
823 Verma, V., Rico-Martinez, R., Kotra, N., King, L., Liu, J., Snell, T. W., and Weber, R. J.:
824 Contribution of water-soluble and insoluble components and their
825 hydrophobic/hydrophilic subfractions to the reactive oxygen species-generating potential
826 of fine ambient aerosols, Environmental science & technology, 46, 11384-11392,
827 10.1021/es302484r, 2012.
828 Verma, V., Fang, T., Xu, L., Peltier, R. E., Russell, A. G., Ng, N. L., and Weber, R. J.: Organic
829 aerosols associated with the generation of reactive oxygen species (ROS) by water-soluble
830 PM2.5, Environmental science & technology, 49, 4646-4656, 10.1021/es505577w, 2015.
831 Wong, J. P. S., Tsagkaraki, M., Tsiodra, I., Mihalopoulos, N., Violaki, K., Kanakidou, M.,
832 Sciare, J., Nenes, A., and Weber, R. J.: Effects of Atmospheric Processing on the Oxidative
833 Potential of Biomass Burning Organic Aerosols, Environmental science & technology, 53,
834 6747-6756, 10.1021/acs.est.9b01034, 2019.
835 Wu, D., Wang, Z., Chen, J., Kong, S., Fu, X., Deng, H., Shao, G., and Wu, G.: Polycyclic
836 aromatic hydrocarbons (PAHs) in atmospheric PM2.5 and PM10 at a coal-based industrial
837 city: Implication for PAH control at industrial agglomeration regions, China, Atmospheric
838 Research, 149, 217-229, 10.1016/j.atmosres.2014.06.012, 2014.
839 Wu, G., Wan, X., Ram, K., Li, P., Liu, B., Yin, Y., Fu, P., Loewen, M., Gao, S., Kang, S.,
840 Kawamura, K., Wang, Y., and Cong, Z.: Light absorption, fluorescence properties and

https://doi.org/10.5194/acp-2021-159
Preprint. Discussion started: 23 February 2021


Atmospheric Chemistry and Physics Discussions

sources of brown carbon aerosols in the Southeast Tibetan Plateau, Environmental pollution, 257, 113616, 10.1016/j.envpol.2019.113616, 2020.

Wu, X., Liu, W., Gao, H., Alfaro, D., Sun, S., Lei, R., Jia, T., and Zheng, M.: Coordinated effects of air pollution control devices on PAH emissions in coal-fired power plants and industrial boilers, The Science of the total environment, 756, 144063, 10.1016/j.scitotenv.2020.144063, 2021.

Yan, C., Zheng, M., Sullivan, A. P., Bosch, C., Desyaterik, Y., Andersson, A., Li, X., Guo, X., Zhou, T., Gustafsson, Ö., and Collett, J. L.: Chemical characteristics and light-absorbing property of water-soluble organic carbon in Beijing: Biomass burning contributions, Atmospheric Environment, 121, 4-12, 10.1016/j.atmosenv.2015.05.005, 2015.

Zhang, X., Lin, Y. H., Surratt, J. D., and Weber, R. J.: Sources, composition and absorption Angstrom exponent of light-absorbing organic components in aerosol extracts from the Los Angeles Basin, Environmental science & technology, 47, 3685-3693, 10.1021/es305047b, 2013.

Zou, C., Li, M., Cao, T., Zhu, M., Fan, X., Peng, S., Song, J., Jiang, B., Jia, W., Yu, C., Song, H., Yu, Z., Li, J., Zhang, G., and Peng, P. a.: Comparison of solid phase extraction methods for the measurement of humic-like substances (HULIS) in atmospheric particles, Atmospheric Environment, 225, 117370, 10.1016/j.atmosenv.2020.117370, 2020.

Open Access
Atmospheric Chemistry and Physics Discussions

860 **Table 1.** The contributions of BrC fraction (WSOC, HULIS, and MSOC) in smoke samples (%).

| | Biomass burning | | | | | | Coal combustion | | | | |
|---|---|---|---|---|---|---|---|---|---|---|---|
| Contents (%) | WS | RS | CS | PW | CR | WP | B-1 | B-2 | B-3 | B-4 | AN |
| OC | 44±5.6 | 41±12 | 24±6.4 | 19±3.8 | 26±8.7 | 23±13 | 61±5.4 | 64±11 | 68±7.6 | 69±6.9 | 9.5±5.0 |
| EC | 2.5±0.9 | 1.3±0.6 | 4.4±2.8 | 10±3.4 | 5.0±3.3 | 13±7.6 | 0.2±0.1 | 1.1±0.8 | 0.3±0.1 | 0.8±0.6 | 0.1±0.0 |
| TC[a] | 46±5.5 | 42±12 | 28±8.2 | 29±4.0 | 32±9.6 | 36±19 | 61±5.4 | 65±11 | 69±6.7 | 69±6.8 | 9.5±5.0 |
| WSOC-C/PM | 11±2.7 | 12±1.6 | 9.7±0.2 | 3.9±1.1 | 7.6±0.3 | 2.9±0.7 | 15±0.4 | 22±4.1 | 9.2±1.5 | 4.7±0.4 | 2.3±1.1 |
| HULIS-C/PM | 6.7±1.3 | 7.8±0.2 | 4.0±0.5 | 1.7±0.3 | 3.1±0.6 | 1.0±0.4 | 6.0±0.6 | 10±0.8 | 4.2±0.4 | 2.0±0.2 | 0.5±0.1 |
| MSOC-C/PM | 40±0.9 | 47±0.8 | 20±1.4 | 12±1.2 | 15±0.9 | 6.4±0.7 | 57±5.4 | 73±2.9 | 65±6.8 | 71±0.7 | 9.4±5.7 |
| WSOC/TC | 22±6.0 | 23±3.0 | 25±3.0 | 14±3.1 | 32±3.0 | 21±9.4 | 25±2.9 | 29±4.3 | 14±3.2 | 6.4±0.5 | 22±8.5 |
| HULIS/TC | 14±2.8 | 14±0.4 | 11±2.7 | 5.9±0.8 | 13±1.6 | 9.8±1.1 | 10±0.3 | 13±1.7 | 6.3±0.9 | 2.8±0.3 | 6.9±2.9 |
| MSOC/TC | 82±2.2 | 88±1.5 | 57±11 | 53±7.5 | 78±16 | 52±27 | 99±0.2 | 95±1.9 | 98±0.1 | 96±0.1 | 95±1.8 |
| HULIS/WSOC | 64±6.9 | 65±8.0 | 42±6.2 | 43±5.4 | 41±6.6 | 32±6.3 | 41±4.9 | 46±9.4 | 46±9. 6 | 43±6.0 | 33±7.8 |
| WSOC/OC | 23±5.9 | 23±3.1 | 33±0.9 | 24±4.0 | 36±2.6 | 35±3.2 | 25±2.9 | 30±4.5 | 14±3.3 | 6.4±0.5 | 26±3.9 |
| HULIS/OC | 15±2.9 | 15±0.4 | 14±1.7 | 10±0.7 | 15±1.9 | 11±3.2 | 10±0.3 | 13±1.6 | 6.4±0.9 | 2.8±0.3 | 6.9±3.0 |
| MSOC/OC | 88±1.9 | 91±1.2 | 70±4.5 | 76±2.5 | 72±6.7 | 77±4.5 | 99±0.1 | 96±0.5 | 98±0.1 | 98±0.5 | 96±1.6 |

861 [a] Total Carbon: sum of OC and EC

862

863

864



https://doi.org/10.5194/acp-2021-159
Preprint. Discussion started: 23 February 2021

865 **Table 2**. The proton species in the BrC fractions (WSOC, HULIS, and MSOC) of smoke samples.

| | | WSOC | | | | HULIS | | | | MSOC | | | |
|---|---|---|---|---|---|---|---|---|---|---|---|---|---|
| | Samples | R-H | H-C-C= | H-C-O | Ar-H | R-H | H-C-C= | H-C-O | Ar-H | R-H | H-C-C= | H-C-O | Ar-H |
| | | 0.6-2.0 [a] | 2.0-3.2 | 3.4-4.4 | 6.5-8.5 | 0.6-2.0 | 2.0-3.2 | 3.4-4.4 | 6.5-8.5 | 0.6-2.0 | 2.0-3.2 | 3.4-4.4 | 6.5-8.5 |
| Biomass burning | WS | 16[b] | 27 | 42 | 14 | 19 | 32 | 21 | 27 | 44 | 26 | 16 | 14 |
| | RS | 24 | 27 | 34 | 14 | 26 | 31 | 14 | 29 | 46 | 30 | 13 | 11 |
| | CS | 15 | 22 | 46 | 17 | 18 | 28 | 31 | 24 | 47 | 29 | 15 | 9 |
| | PW | 14 | 22 | 48 | 17 | 15 | 25 | 42 | 18 | 40 | 30 | 19 | 11 |
| | CF | 11 | 17 | 54 | 18 | 14 | 26 | 36 | 23 | 41 | 28 | 18 | 13 |
| | WP | 12 | 22 | 48 | 19 | 14 | 21 | 31 | 34 | 44 | 29 | 17 | 10 |
| Coal combustion | B-1 | 18 | 41 | 9.0 | 32 | 17 | 40 | 5.0 | 37 | 40 | 28 | 2.0 | 30 |
| | B-2 | 17 | 35 | 22 | 25 | 26 | 39 | 5.0 | 30 | 33 | 30 | 3.0 | 33 |
| | B-3 | 17 | 39 | 14 | 30 | 22 | 34 | 8.0 | 35 | 34 | 30 | 2.0 | 33 |
| | B-4 | 13 | 27 | 34 | 25 | 20 | 36 | 13 | 30 | 32 | 27 | 3.0 | 39 |
| | AN | 15 | 33 | 20 | 32 | 18 | 37 | 12 | 33 | 38 | 28 | 2.0 | 32 |

866 [a] chemical shift: ppm. [b] percentage of each type of protons (%).

867



https://doi.org/10.5194/acp-2021-159
Preprint. Discussion started: 23 February 2021

https://doi.org/10.5194/acp-2021-159
Preprint. Discussion started: 23 February 2021


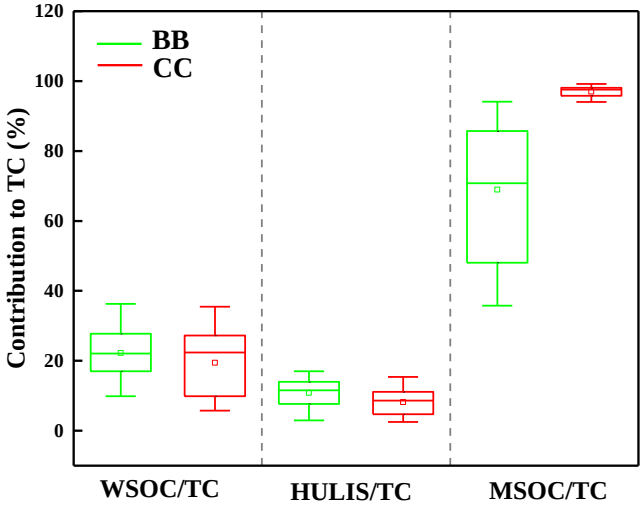


**Figure 1.** The abundances of BrC fraction in the smoke samples from biomass burning (BB) and coal combustion (CC)

https://doi.org/10.5194/acp-2021-159
Preprint. Discussion started: 23 February 2021


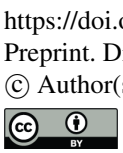

Atmospheric Chemistry and Physics Discussions

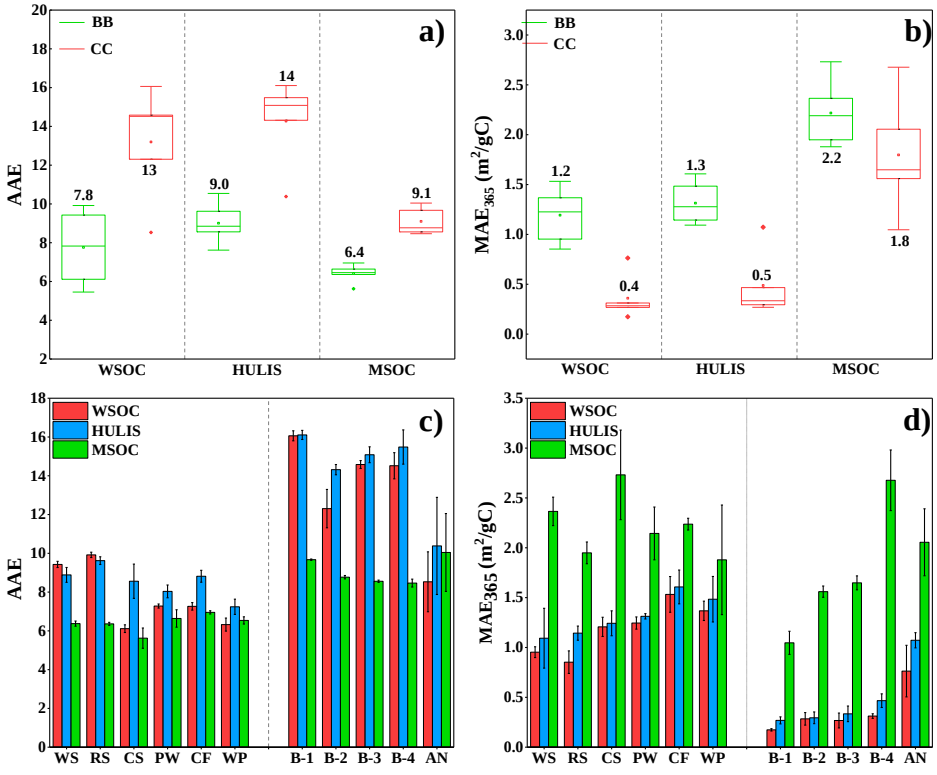


**Figure 2.** The AAE and $MAE_{365}$ values of WSOC, HULIS, and MSOC in smoke samples from biomass burning (BB) and coal combustion (CC)

https://doi.org/10.5194/acp-2021-159
Preprint. Discussion started: 23 February 2021


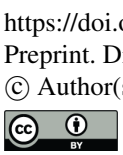

Atmospheric Chemistry and Physics Discussions

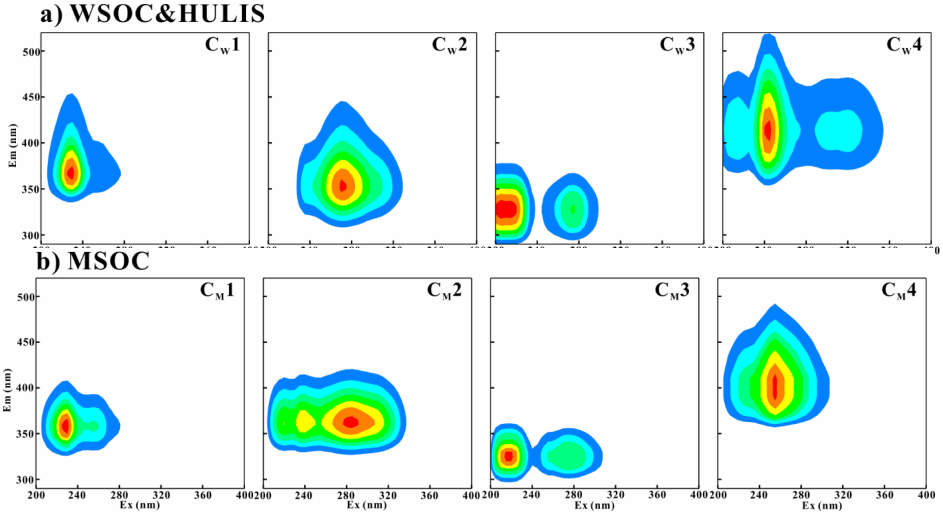


**Figure 3.** Four fluorescence components identified by PARAFAC analysis of a) WSOC, HULIS ($C_W1$:$C_W4$); b) MSOC ($C_M1$:$C_M4$) extracted from BB and CC smoke $PM_{2.5}$ (normalized in Raman unit, R.U.)

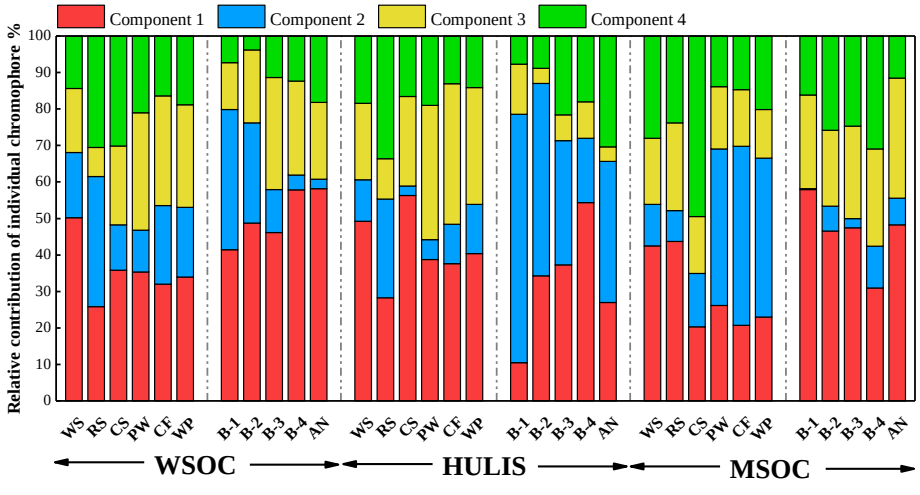


**Figure 4.** Relative contribution calculated by $F_{max}$ of individual chromophores analyzed by PARAFAC. Component 1-4 represent $C_W1$-4 for water-soluble BrC (WSOC and HULIS) and and $C_M1$-4 for methanol-soluble BrC (MSOC), respectively.

https://doi.org/10.5194/acp-2021-159
Preprint. Discussion started: 23 February 2021


Atmospheric Chemistry and Physics Discussions

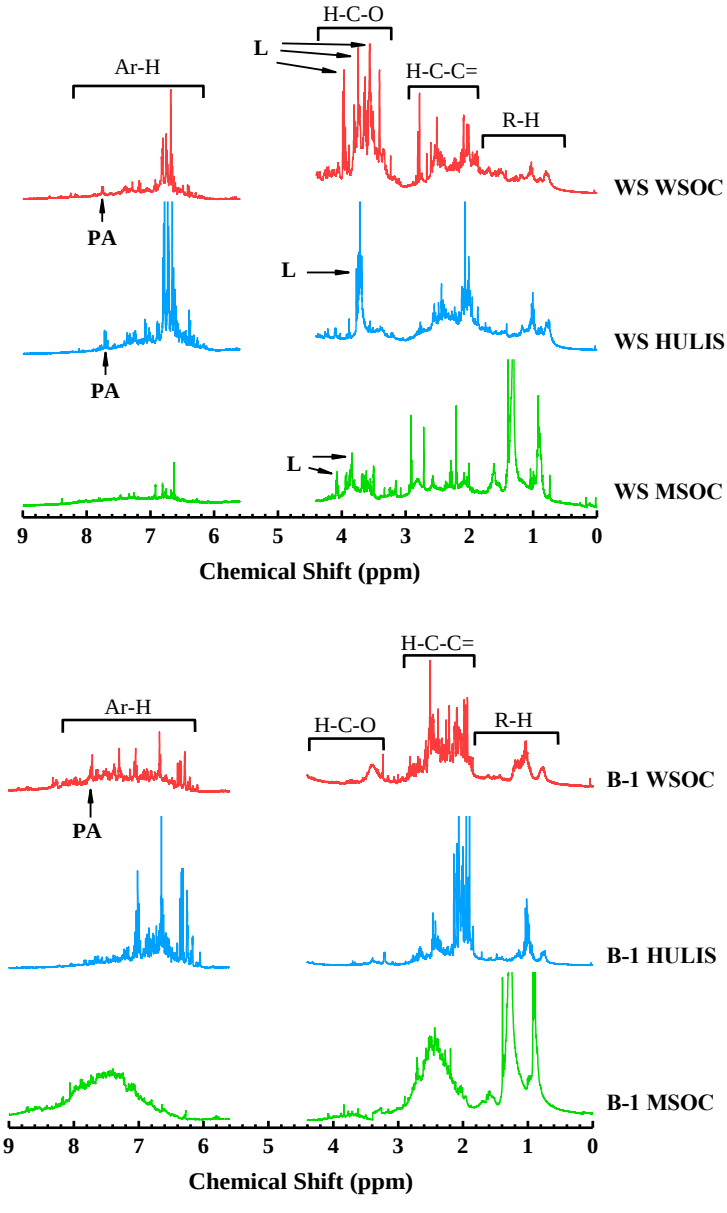


**Figure 5.** $^{1}$H NMR spectra of WSOC, HULIS, and MSOC in typical biomass burning (WS) and coal combustion (B-1) smoke samples. The segment from 4.40 to 5.60 ppm was removed for NMR spectra due to MeOH and $H_2O$ residues. The peaks were assigned to specific compounds as follows: Levoglucosan (L), Phthlic acid (PA).

https://doi.org/10.5194/acp-2021-159
Preprint. Discussion started: 23 February 2021


Atmospheric Chemistry and Physics Discussions

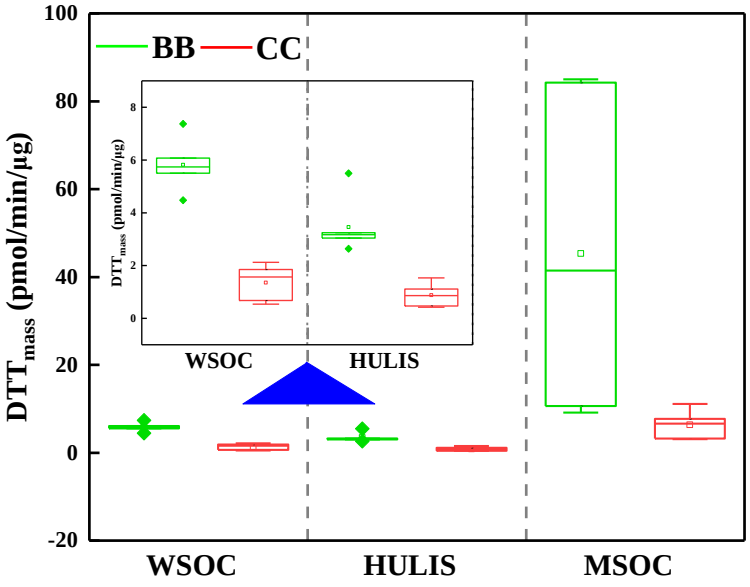


**Figure 6.** Results of DTT assay conducted on the WSOC, HULIS and MSOC of smoke $PM_{2.5}$, the value were normalized by smoke $PM_{2.5}$ mass. Above the blue triangle symbol is the result coordinates of WSOC and HULIS to be enlarged.